Rendiconti Lincei. Scienze Fisiche e Naturali (2019) 30:497–513
https://doi.org/10.1007/s12210-019-00830-8

SOLAR DRIVEN CHEMISTRY

Metal-free carbon-based materials for electrocatalytic and photo-electrocatalytic CO_2 reduction

Nicola Sangiorgi[1] · Giulia Tuci[2] · Alessandra Sanson[1] · Maurizio Peruzzini[2] · Giuliano Giambastiani[2,3]

Received: 3 June 2019 / Accepted: 15 July 2019 / Published online: 24 July 2019

Abstract

Nowadays, reducing carbon dioxide emission in the atmosphere is one of the most important environmental issues that must be overcome. At the same time, low-cost and environmentally friendly technologies are necessary to produce renewable fuels able to replace the conventional fossil ones. Electrochemical cells (driven by solar energy) and photo-electrochemical cells (PECs) are among the main efficient technologies to get these challenging goals. Taking into account the PEC working mechanism, two different electrodes, based on photo-electrocatalytic and electrocatalytic materials able to drive reactions both under illumination or in dark conditions, are involved. In this review, recent results on carbon-based materials for electrocatalytic and photo-electrocatalytic carbon dioxide reduction are discussed. The properties and synthesis conditions applied to the preparation of conducting polymer and graphitic carbon nitride (g-C_3N_4) are described and discussed for their application in the photoactive electrodes. As for the electrodes to be applied in the electrocatalytic CO_2 activation and conversion, light heteroelement-doped carbon nanomaterials have been taken into account as highly valuable metal-free candidate to run the process efficiently and selectively. For the latter process, also the influence of the electrolyte and the selectivity towards different reaction products will be discussed. All these data taken together indicate that a lot of work still has to be done to achieve high efficiency with metal-free organic-based electro- and photo-electrocatalysts applied to the carbon dioxide conversion. Anyhow, many seminal outcomes collected in the literature up to now clearly indicate the real possibility to replace highly costly metal-based materials with simply organic ones.

Keywords Metal-free electrodes · Carbon-based materials · Electrocatalysts and photoelectrocatalysts · Carbon dioxide conversion · Photoelectrochemical cell · Products selectivity

1 Introduction

Energy demand, in the context of increasing global population and energy consumption, combined with steady reduced supply of traditional fossil fuels sources and the effect of carbon dioxide emissions on environmental and climate changes, represents a key issue of our modern society. The research of alternative renewable energy sources to power our planet and the development of new technologies applied to the reduction of carbon dioxide concentration in the atmosphere are among the most urgent priorities to be urgently addressed. In this scenario, CO_2 activation and catalytic conversion represents a highly attractive approach for harvesting a greenhouse gas and a chemical "waste" and converting it into chemicals and fuels of added value. Among the possible methods for CO_2 conversion, (photo) electro-reduction holds great potentialities (Kalamaras et al. 2018; Wang et al. 2018a; Chang et al. 2016; Duan et al.

This contribution is the written, peer-reviewed version of a series of papers presented on the occasion of the International Conference on "Solar driven chemistry: towards new catalytic solutions for a sustainable world", held at Accademia Nazionale dei Lincei in Rome on 18–19 October 2018.

✉ Nicola Sangiorgi
nicola.sangiorgi@istec.cnr.it

✉ Giulia Tuci
giulia.tuci@iccom.cnr.it

[1] Institute of Science and Technology for Ceramics, ISTEC-CNR, Via Granarolo 64, 48018 Faenza, RA, Italy

[2] Institute of Chemistry of OrganoMetallic Compounds, ICCOM-CNR, Via Madonna del Piano 10, 50019 Sesto Fiorentino, FI, Italy

[3] Institute of Chemistry and Processes for Energy, Environmental and Health (ICPEES), ECPM, UMR 7515 of the CNRS-University of Strasbourg, 25 Rue Becquerel, 67087 Strasbourg Cedex 02, France

2017; Liu et al. 2017a). Indeed, with respect to other and more energy consuming technologies [i.e., biological and biochemical transformations (enzyme or algae based), thermochemical conversion and mineralization] (Zheng et al. 2017), CO_2 (photo)electro-reduction lists several advantages such as an effective control on the reaction products by tuning the experimental parameters (i.e., temperature, electrolyte, applied potential, etc.) and mild operative conditions both in terms of reaction temperature and gas pressure. In addition, CO_2 reduction by PEC systems is directly driven by solar energy that is the most abundant (about 10^5 TW supplied on Earth's surface every year) renewable energy source available. As a matter of fact, the production of fuels and chemicals from the "photo-induced" reduction of carbon dioxide is a challenging technology and a valuable route to store intermittent renewable energy in an accessible format, while employing current infrastructures (Armaroli and Balzani 2016). Three different configurations for PEC carbon dioxide reduction have been used up to date: photocathode-driven PEC, photoanode-driven PEC and combined photoanode and photocathode (Z-scheme, artificial photosynthesis) cells (Kalamaras et al. 2018; Wang et al. 2018b; Yang et al. 2018; Xie et al. 2016). Thermodynamic and kinetic aspects need to be considered into PEC technology because the reaction rate and products can be controlled through the applied external potential as well as the nature of the catalyst used. Moreover, the kinetic largely depends on other factors such as the reaction temperature and pressure, the reagents concentration and the electrolyte (Xie et al. 2016). At the same time, to produce highly efficient PEC systems, the reactor design must be taken into account as well as the carbon dioxide adsorption and activation mechanism. However, due to the complexity of processes occurring inside a PEC system, it is a critical issue to understand the CO_2 adsorption and conversion route on the electrode materials for the realization of highly efficient PEC technology (Kalamaras et al. 2018; Chang et al. 2016; Yang et al. 2018).

A PEC system for carbon dioxide conversion is characterized by two solar-driven reactions (reduction and oxidation) on the electrodes separated by an electrolyte. The electrodes can work in dark condition (dark electrode) or under illumination (photoelectrode) in the presence of a current collector (Wang et al. 2018a; Yang et al. 2018). Typically, a transparent conductive substrate (fluorine or indium doped tin oxide) is used for the photoelectrode preparation due to its electrical and transparent properties. The space between the electrodes is filled with the electrolyte solution where the reagents are bubbled and, to achieve highly efficient devices, a separation membrane selective for H^+ migration (such as Nafion) is used for products separation. A stirring system is also required to ensure a good mass diffusion for both the reagents and the products. A reference electrode is finally used for determining potential during PEC tests. Materials with different properties are used for the realization of the three different PEC configurations previously described and reported in Fig. 1.

For the photoanode-driven PEC (Fig. 1a), an active material based on a n-type semiconductor (with an excess of electrons on the conduction band) is required. When the sunlight reaches the semiconductor with a photon of energy equal or higher than the band gap energy (E_g), it creates positive and negative charges (holes and electrons) on its valence (V_B) and conduction bands (C_B), respectively. Due to the n-type semiconductivity, the photogenerated holes can oxidize water; while, the electrons reach the cathode under dark conditions. The water oxidation reaction produces H^+ ions that selectively move to the compartment where the carbon dioxide is added reducing it into useful products and fuels that can be easily separated. Conversely, a semiconductor material with p-type properties (an excess of holes are present on its valence band) is considered in a photocathode-driven PEC (Fig. 1b). Now, the photogenerated electrons and holes are used to drive water oxidation reaction and carbon dioxide as in the previous case, but the holes are used to produce H^+ at the dark side; while, the electrons are used to produce solar fuels and products at the photocathode. Finally, to mimic the photosynthetic process, both photoelectrodes can be illuminated and generate simultaneously the electron–hole pairs (Fig. 1c). The majority of the photogenerated charges are recombined at the ohmic contact between the two electrodes and only some charges carriers can be used for oxidation and reduction reactions. However, this is the most promising approach for the development of the next generation PEC due to the possibility to drive the different reactions without applying an external potential. Taking into account Fig. 1 (in particular Fig. 1a, b), the CO_2 conversion occurs by electrocatalytic reactions both under illumination (on photocathode side) and dark conditions (on cathode side). For this reason, the properties of electrode materials for photo-electrocatalytic and electrocatalytic CO_2 conversion (CO_2RR) are key parameters for the development of highly efficient PEC system.

The development of efficient (photo)-electrocatalytic materials for carbon dioxide conversion is a difficult task due to the high thermodynamic stability and chemical inertness of CO_2 (Ponnurangam et al. 2017). Moreover, multiple-electron process is required, involving from 2 up to 12 electrons, thus potentially leading to a large variety of C1 and/or C2 products (Table 1). An accurate control of the process selectivity is, therefore, one of the major challenges in this research field that has not been fully addressed yet (Kalamaras et al. 2018; Chang et al. 2016; Duan et al. 2017; Yang et al. 2018). In addition, when aqueous electrolytes are used, hydrogen evolution reaction (HER) arises as a highly competitive process (Table 1), potentially lowering

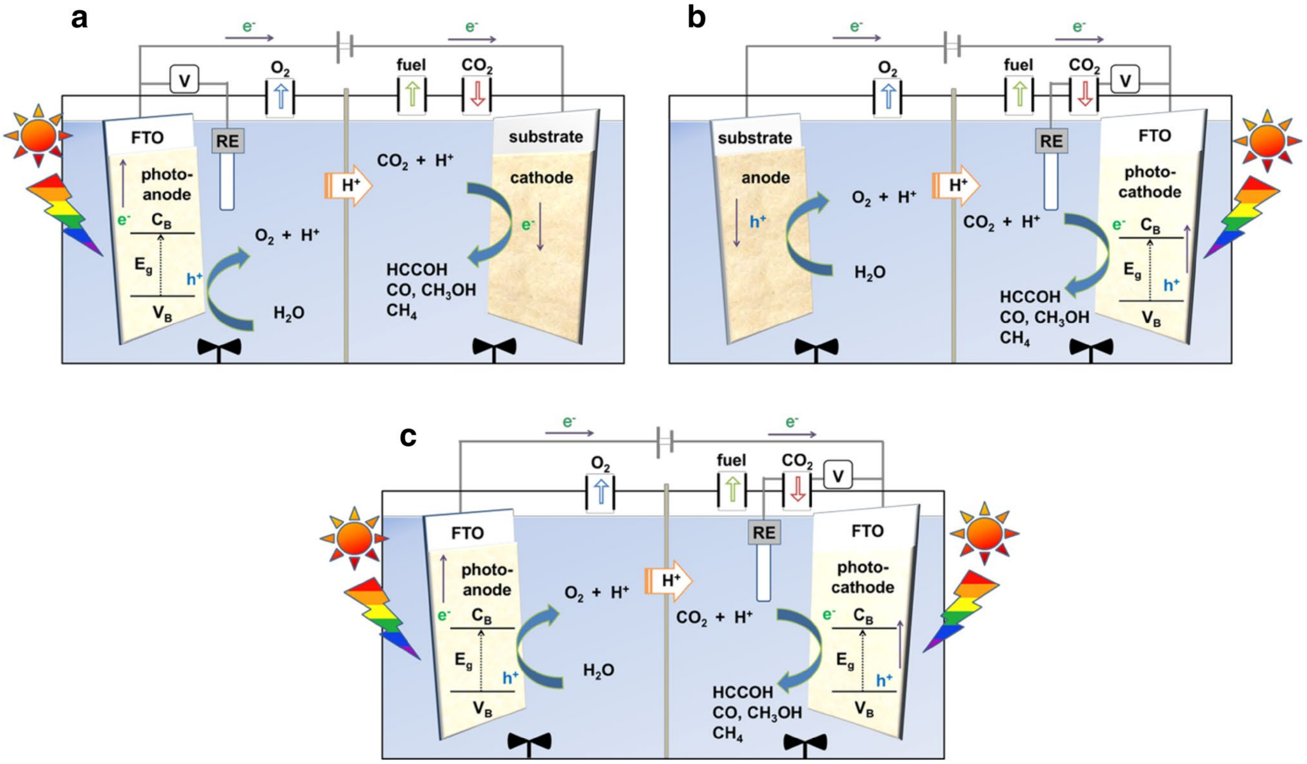

Fig. 1 Schematic illustration of the possible PEC configuration with 2 compartment cells: **a** photoanode driven; **b** photocathode driven and **c** with photoanode and photocathode driven

Table 1 Standard potential for water splitting and carbon dioxide reduction reactions

Reaction	$E°$ (V) vs NHE at pH 0
$2H^+ + 2e^- \rightarrow 2H_2$	0
$2H_2O \rightarrow 4H^+ + O_2 + 4e^-$	− 1.23
$CO_2 + e^- \rightarrow CO_2^{-}$	− 1.90
$CO_2 + 2H^+ + 2e^- \rightarrow HCOOH$	− 0.20
$CO_2 + 2H^+ + 2e^- \rightarrow CO + H_2O$	− 0.11
$CO_2 + 4H^+ + 4e^- \rightarrow H_2CO + H_2O$	− 0.07
$CO_2 + 6H^+ + 6e^- \rightarrow CH_3OH + H_2O$	0.03
$2CO_2 + 12H^+ + 12e^- \rightarrow C_2H_4 + 3H_2O$	0.08
$2CO_2 + 12H^+ + 12e^- \rightarrow C_2H_5OH + 3H_2O$	0.08
$2CO_2 + 14H^+ + 14e^- \rightarrow C_2H_6 + 2H_2O$	0.14
$CO_2 + 8H^+ + 8e^- \rightarrow CH_4 + 2H_2O$	0.17

the overall catalytic efficiency. As a result, the ambitious goal of this research area is to design and develop efficient (photo)-electrocatalysts able to maximize CO_2 conversion towards a target product, while suppressing undesired side processes.

Several metal-based heterogeneous catalysts have been reported to date as valuable promoters for both PEC and CO_2RR. Anyway, they irremediably suffer from common drawbacks such as poor sustainability (from an environmental and economical view-point), scarce selectivity and fast deactivation due to poisoning/leaching or photo-corrosion phenomena. As cheap, environmentally benign and effective alternatives to CO_2 (photo)electro-reduction, metal-free carbon-based materials have been extensively investigated in the last years (Cui et al. 2018), showing often comparable, and to some extent better, catalytic performance with respect to metal-based systems. The importance of this topi was highlighted in a very recenlty special issue on Advanced Materials named “Carbon-based metal-free catalysts (2019)”.

This review aims at highlighting the recent achievements in PEC and CO_2RR processes promoted by metal-free carbon-based materials. Despite that metal-free technologies applied to CO_2 conversion and valorization into commodities and fuels of added value are relatively new, this research field has already scored many interesting results. However, several aspects such as selectivity, productivity and the controversial relationships between structure and performances of carbon-based materials are still pending issues that will be discussed within this review.

2 Photo-electrocatalytic (PEC) CO_2 reduction

PEC photoelectrodes for carbon dioxide reduction based on organic semiconductors have attracted great attention due to their unique advantages such as low cost, high abundance, environmental friendliness and high charge-carrier mobility (Yao et al. 2018; Hursán et al. 2016). Moreover, organic semiconductors are more stable than the metal-based ones in water and under photo-electrochemical conditions because not influenced by photo-corrosion phenomena. These properties reduce also their payback time as well as the EROI parameter (energy returned of investment). In this review, photoelectrodes for CO_2 conversion based on organic semiconductors thin films are considered as primary light harvesting and charge-transport materials. Conducting polymers (CPs) and graphene-like carbon nitride (g-C_3N_4) were considered, because they can be easily prepared and deposited on the electrode surface as thin films and their optical and electronic properties are suitable for CO_2 conversion within PEC systems. Other organic semiconductor such as graphene, conjugated polymers and materials for organic photovoltaics (OPV) were not taken into account as they are not yet considered due to their low limitation in PEC for CO_2 conversion even if these materials found application in the photocatalytic and photo-electrochemical water splitting applications and photocatalytic carbon dioxide reduction. A deep overview on their properties can be found in different reviews (Yao et al. 2018; Remiro-Buenamañana and García 2019; Joy et al. 2018; Zhang et al. 2018a).

2.1 Conducting polymers (CP)

Conducting polymers (CPS) are a class of organic materials characterized by particular electronic properties such as definite band gap energy and enhanced electronic conduction (Yongfang 2015; Dai 2004). For carbon dioxide reduction in PEC systems, three are three compounds most commonly used: polyaniline, polypyrrole and poly(3,4-ethylenedioxythiophene) (PEDOT), due to their lower overpotential generally required for the electrocatalytic carbon dioxide reduction compared with metal-based catalytic systems. Other CPs such as polythiophene, are considered only for water splitting reaction and are not therefore interesting for this work (Fan et al. 2016; Kao et al. 2018). The monomer chemical structures of the three abovementioned CPs are reported in Fig. 2.

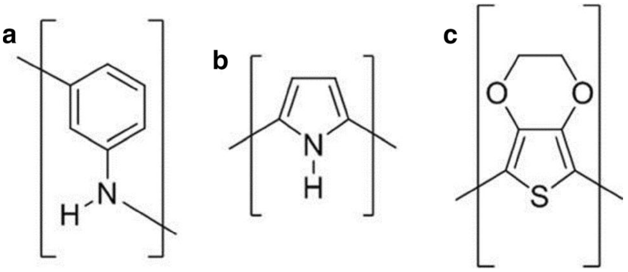

Fig. 2 Chemical structures of monomers for CPs considered for CO_2 PEC technology: **a** aniline, **b** pyrrole and **c** 3,4-ethylenedioxythiophene

Each system is characterized by the presence of heteroatoms (nitrogen, sulphur and oxygen) that can contribute significantly to the electrochemical reduction of carbon dioxide (Li et al. 2017a; Smith and Pickup 2010). Both nitrogen (pyridinic and quaternary) and sulphur induce the formation of positive charge on the polymeric chain that can play an important role in the CO_2 reduction. In this condition, however, the hydrogen evolution reaction can also take place and compete with carbon dioxide reduction. The presence of pyridinic-N, in particular, stabilizes the CO_2^-/*COOH intermediate, that represents an important step for the CO formation (Li et al. 2017b; Li and Bandosz 2018). Besides these chemical properties, CPs electronic properties allow the application of these materials as PEC photoelectrodes. In fact, CPs are widely used for energy production and storage, sensors and separation techniques due to their high conductivity (10^{-3}–10^3 S/cm), low cost, good stability and high catalytic activity towards a lot of different reactions and redox properties (Yongfang 2015; Sangiorgi and Sanson 2017; Sangiorgi et al. 2019). In addition, CPs have many other interesting characteristics for energy application such as transparency, flexibility, easy availability and low-cost deposition processes (such as electropolymerization). CPs possess the electronic and optical properties of metal inorganic semiconductors but at the same time the flexibility and mechanical properties of polymers (Dai 2004). The distinctive properties of CPs are related to the conjugated molecular structure of the polymeric main chain, where π-electrons are delocalized over the whole polymer. For this reason, these materials exhibit the well-known band structure with π-valence band and π*-conduction band (valence band and the conduction band, respectively). The difference in energy between the valence band and the conduction band (the highest occupied molecular orbital, HOMO, and the lowest non-occupied molecular orbital LUMO, respectively) is the band gap energy that normally stands in the 1.5–3.0 eV range, therefore suitable for absorbing photon energy. The conductivity of CPs can be manipulated by doping during their synthesis. In fact, the charges can flow on them, thanks to the presence of polarons, bipolarons or solitons (degenerated polymers based on two equivalent resonance forms) delocalized on conjugated polymer chain produced after oxidation and reduction doping process (Yongfang 2015; Dai 2004). Via doping process, the conjugated polymers can, therefore, become p- or n- type conductors. In the p-doped state, the main chain is oxidized with a counter-anion that keeps the electron neutrality of the molecule balancing the holes created in the main chains. In the n-doped state, the main chain of the CP is reduced with a counter-cation that helps to maintain the electron neutrality balancing the electrons in the main chains (Yongfang 2015). These types of doping processes can be achieved by two main methods: chemical or electrochemical.

One of the most interesting applications of CPs in PEC technology is the use of polyaniline photocathode to reduce CO_2 to alcohols (Hursán et al. 2016). Polyaniline can in fact photochemically reduce carbon dioxide without adding specific catalysts also as a consequence of a surface with good selectivity for chemical interaction with CO_2. This is due to the N-rich polymeric chains that are generally considered as the best solid-state adsorbents for CO_2. PANI films were prepared by electrochemical polymerization on gold electrode. Under illumination (300 W Xe–Hg arc lamp) and with CO_2-saturated electrolyte, PANI electrode shows a cathodic photocurrent equal to 170 µA/cm^2 instead of the 80 µA/cm^2 obtained with nitrogen-saturated electrolyte. When the PANI was prepared with MWCNTs as substrate, the photocurrent reaches 0.5 mA/cm^2 due to the improved charge separation and transport processes (Fig. 3). Electrolysis tests under potentiostatic conditions with CO_2 were done with an applied potential of − 0.4 V vs Ag/AgCl (NaCl 3 M) and the acquired stationary photocurrent after 7000 s was equal to 70 µA. In these conditions, the obtained products were methanol and ethanol (with H_2 present in gas phase) with a Faradic efficiency equal to 43% and 20%, respectively. The comparison between PANI photoelectrodes and the ones based on polypyrrole (PPy) and PEDOT (prepared by electrochemical polymerization) confirms that the nitrogen atoms present inside the polymers were found to control the photo-electrochemical CO_2 reduction affecting its final conversion.

For PEDOT and PPy, where the N-rich polymeric chain is less available (PPy) or not present (PEDOT) ,the

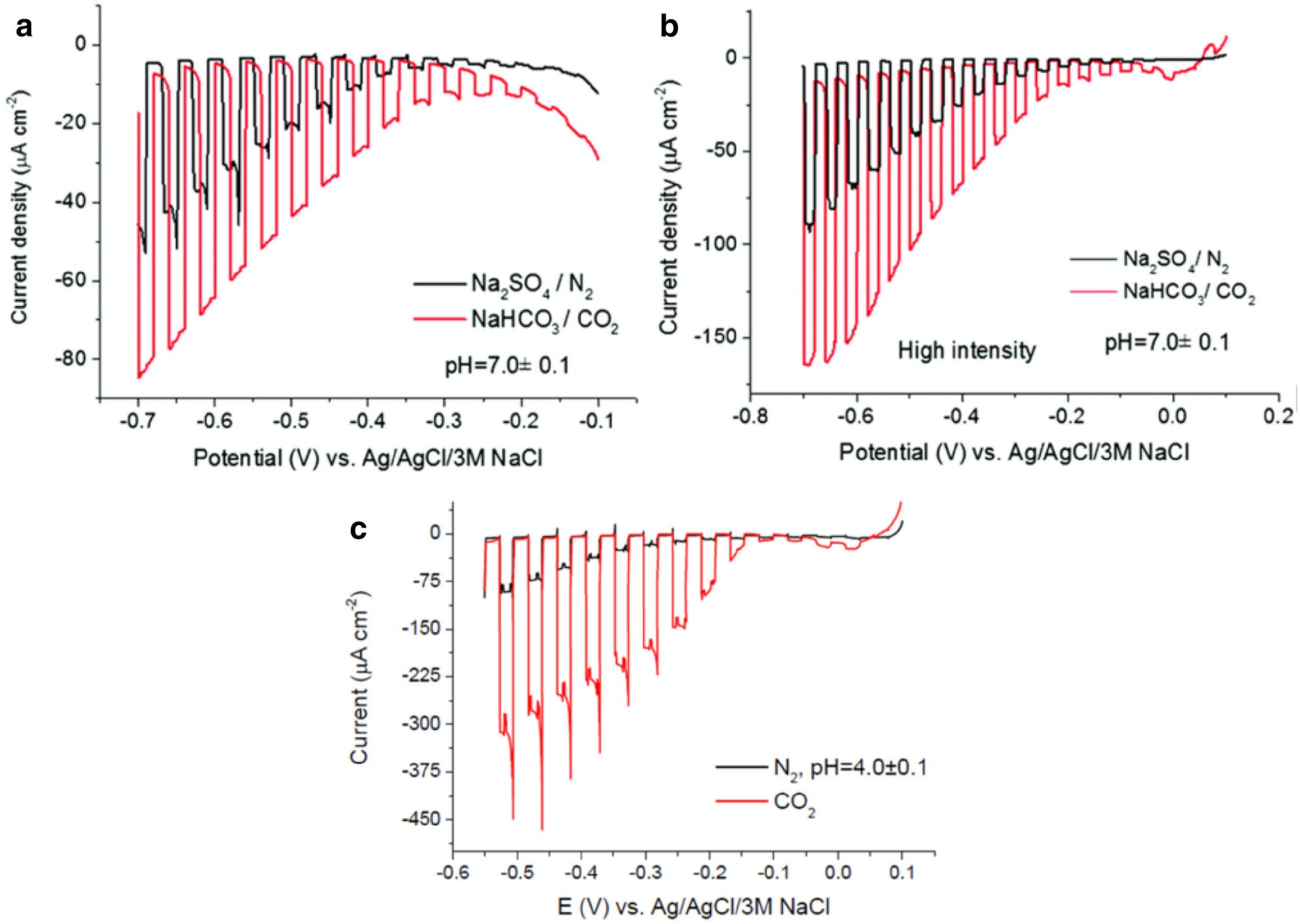

Fig. 3 Photocurrent acquired for PANI electrodes under **a** low (100 W) and **b** high (300 W) illumination conditions at pH 7.0 and **c** related to PANI/MWCNTs under 300 W at pH 4.0. Adapted from Hursán et al. (2016) with permission from The Royal Society of Chemistry

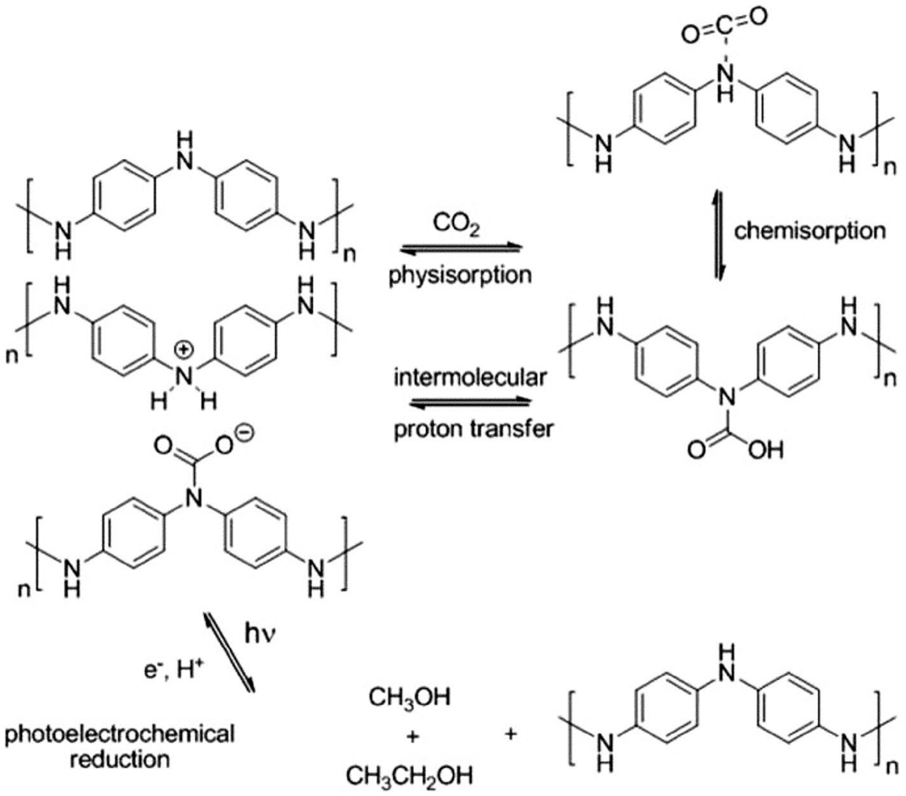

Fig. 4 Proposed mechanism for carbon dioxide adsorption and photo-electrochemical reduction on PANI electrode. Reproduced from Hursán et al. (2016) with permission from The Royal Society of Chemistry

photocatalytic activity was found to be definitively lower. Hursán et al. (2016) proposed a dedicated mechanism for the interaction between PANI and CO_2 (Fig. 4).

Kormányos et al. (2017) reported the application of PANI electrodes for solar fuels production and described the properties of the nanohybrid photoelectrodes based on PANI/SiC. The polymer was prepared by electrochemical method (potentiodymanic cycling) producing a PANI film with band gap energy of 2.9 eV suitable for harvesting visible portion of the light spectrum. Moreover, PANI was able to reduce CO_2 photo-chemically (under 300 W Hg–Xe arc lamp) producing a correspondent photocurrent of 15 µA/cm^2 (in CO_2-saturated $NaHCO_3$ 0.1 M solution). The performances of PANI considerably enhanced when used in combination with SiC. The photocurrent obtained with the hybrid (PANI/SiC) electrode was in fact doubled with respect to that obtained with the plain PANI. The influence of PANI film thickness was studied changing the amount of current applied on the electrode during the electro-polymerization process and the highest photocurrent (150 µA/cm^2) was obtained with the highest amount of polymer deposited (40 mC/cm^2). The electrolysis tests on CO_2 photoreduction show the presence of H_2 and CO in the case of plain PANI electrode; while for PANI/SiC, the same amount of H_2 together with a higher amount of CO and a small quantity of methanol and ethanol were found. The enhancement of photocurrent was mainly due to the higher specific surface area of PANI/SiC electrode and the positive catalytic effect of PANI on electrons transfer from SiC to the substrate. Other than PANI, polypyrrole (PPy) films were used as efficient photoelectrode for solar fuels production (Beladed et al. 2013; Won et al. 2015). Beladed et al. (2013) reported PPy prepared by chemical synthesis showing a direct band gap energy of 1.02 eV and p-type conductivity properties with energy levels suitable for photocathode application in PEC technology. The obtained E_g shows the ability of PPy to absorb the visible part of the solar spectrum. Stability tests were done (under 200 W lamp) in different pH conditions and the results show the high stability of PPy electrodes to corrosion phenomena. In the paper by Won et al. (2015), PPy was prepared by electrochemical polymerization (cyclic voltammetry) controlling the film thickness with the amount of charges that flow on the metal electrode during the synthesis. The PPy films were able to reduce CO_2 to formic acid (under 450 W Xe lamp) at -0.3 V vs RHE of applied potential with 21.1% Faradic efficiency. This value was improved by using 40-nm PPy film electropolymerized on p-type ZnTe substrate. The composite electrode reaches at -0.2 V vs RHE the Faradic efficiencies of 37.2% and 13.8% for formic acid and carbon monoxide, respectively. The production rates were 0.11 and 0.04 µmol h^{-1} cm^{-2} for formic acid and carbon monoxide, twice the values obtained for bare ZnTe photocathode. In these conditions, also hydrogen was detected as co-product but in a minor extent compared to bare ZnTe. The positive effect of PPy on ZnTe properties was due to the decrease of electron–hole recombination on the interface PPy/ZnTe (observed by electrochemical impedance experiments) and the corresponding improvement of the electron transfer. The presence of PPy enhances the selectivity on formic acid production and the polymer reduces the recombination of surface adsorbed protons. Finally, only few articles report the application of poly(3,4-ethylenedioxythiophene) (PEDOT) as photoelectrode for PEC application (Hursán et al. 2016; Ghosh et al. 2018). Ghosh et al. (2018) studied the properties of PEDOT nanofibers prepared by chemical polymerization and the influence of gold nanoparticles (Au NPs) added to PEDOT for the realization of new nanohybrid photoelectrochemical active material. During the linear sweep voltammetry (LSV) analyses, the bare PEDOT photoelectrode was able to produce a photocurrent of 3.9 ± 0.05 mA/cm^2 at potential of 0.8 V vs Ag/AgCl under visible light irradiation (100 mW/cm^2). On the other hand, when the nanohybrid PEDOT/Au NPs electrode was tested in the same conditions, the photocurrent was enhanced to 11.2 ± 0.09 mA/cm^2 reducing the onset potential if compared with bare PEDOT. The stability tests performed on the nanohybrid electrodes show high stability with degradation of just 8% after 240 min. The highest performance obtained for PEDOT/Au NPs was due to the properties of the interface created between these two materials that enhanced the light harvesting, thanks to the co-sensitization of plasmonic Au NPs by multiple states of PEDOT coming from the oligomeric and polymer chain unit. In general, CPs possess a great potential for their application as photoelectrode in PEC systems for CO_2 conversion, but their electronic and catalytic properties must be further enhanced to make this materials competitive with the metal-based ones.

2.2 Graphitic carbon nitride

Graphitic carbon nitride (g-C_3N_4) represents an emerging polymeric semiconductor suitable for solar fuels production. In particular, a lot of work has been devoted to photocatalytic, electrocatalytic and photoelectrochemical hydrogen production; while, an enormous interest for carbon dioxide reduction has recently emerged (Volokh et al. 2019; Wang et al. 2018b; Shen et al. 2018; Lu et al. 2018; Sun et al. 2018; Fang et al. 2018a; Cao et al. 2017; Wen et al. 2017; Ma et al. 2018; Dong et al. 2016; Fang and Wang 2018; Fang et al. 2018b). g-C_3N_4 is a 2D material constituted by a single-layer of *sp*^{2} hybridized graphitic nanosheets based on carbon and nitrogen atoms bound by van der Waals forces. Moreover, g-C_3N_4 is composed of two cheap, abundant, biocompatible and nontoxic elements with a stable structure based on tri-s-triazine amino rings as the basic units and a minor amount of residual amino groups on the edge of the structure. The chemical structure of g-C_3N_4 is reported in Fig. 5.

Figure 5 shows the presence of a nitrogen-rich structure that is suitable for adsorption and activation of a high amount of carbon dioxide. In particular, the triazine nitrogen and amino groups act as Lewis and Brönsted basic sites that are expected to favor carbon dioxide capture and activation. Moreover, the 2D structure can facilitate the electron transfer during the photo-electrochemical reaction and the tunable structure can be modified by changing the precursors and polymerization conditions. Wang et al. (2009) reported C_B and V_B levels at -1.3 V and $+1.6$ V vs NHE at pH 7 indicating the great potentiality of this material for carbon dioxide photocatalytic reduction. The high negative energy position of C_B suggests that the photogenerated electrons possess a high thermodynamic driving force to reduce water, oxygen and carbon dioxide. About CO_2 reduction mechanism, the activation of carbon dioxide was one of the most important step that influences the overall final efficiency. Goettmann et al. (2007) showed the ability of g-C_3N_4 material to reduce CO_2 to CO and recently, Azofora et al. (2016) and Zhu et al. (2017) performed DFT experiments to deeply understand the photocatalytic mechanism. Low Gibbs free energy for the first reaction (H^+/e^-) was found for the corrugate g-C_3N_4 with respect to the planar structure, thanks to a reduced electronic repulsion. Moreover, the corrugate structure was found to be selective for the production of CO/CH_3OH. DFT analyses demonstrated that CO_2 molecules adsorb preferably at the two-coordinated N atom instead of the other nitrogen groups. Finally, the band gap value was found to be around

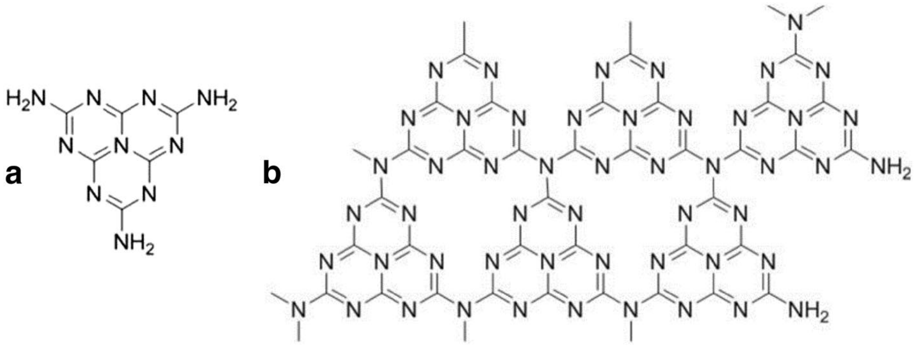

Fig. 5 Structures of **a** tris-s-triazine as the building block of **b** g-C_3N_4 structure

2.7 eV (corresponding to a wavelength of 460 nm), therefore suitable to capture a portion of visible sunlight. The light absorption process occurs by π–π* transition in the conjugated aromatic structure. The g-C_3N_4 can be easily synthesized through polymerization processes of different nitrogen-rich precursors such as melamine, dicyanamide, cyanamide urea and thiourea. On the other hand, the g-C_3N_4 nanosheets should be prepared by an exfoliation procedure from the bulk material (Volokh et al. 2019; Wang et al. 2018a). The precursors and the synthesis approach deeply influence the final properties of the g-C_3N_4 in terms of energy band position, defects, surface area and electronic properties. Thanks to these properties, as described before, a lot of papers and reviews were dedicated to the use of g-C_3N_4 for water splitting reaction and carbon dioxide reduction. In this work only the use of g-C_3N_4 as thin film for PEC application will be discussed. Nowadays, the preparation of high quality g-C_3N_4 film represents one of the main issue for the development of highly efficient PEC systems for carbon dioxide reduction based on this material (Volokh et al. 2019). In fact, normally the g-C_3N_4 is obtained as a powder or in the bulk form that do not allow to obtain films with suitable photoelectrode properties (good substrate adhesion, good electrical connection and electron transport, homogeneity, continuity, stability). To overcome this issue, very promising results were obtained considering a bottom–up approach to prepare the g-C_3N_4 film directly on the substrate. Wang et al. (2018b) reported an accurate review on the different deposition processes. Focusing on carbon dioxide reduction driven by PEC processes, Saraga et al. (2016) studied the properties of g-C_3N_4 thin film and the influence of doping with boron. Considering the n-type semiconductivity, g-C_3N_4 was doped with different boron content (0.5–1.5–3.0 at%) and the as-obtained materials were deposited on FTO (fluorine doped tin oxide) substrate by electrophoretic deposition. For all the samples prepared, the absorption edge was found around 550 nm and the corresponding band gap energy for the sample with boron at 1.5 at% was 2.59 eV. Moreover, thanks to the doping effects, the semiconductivity was changed and the B-doped g-C_3N_4 samples show a p-type conductivity. Mott–Schottky analyses in $NaHCO_3$ 0.5 M solution (pH 8.6) show a flat band potential for B-doped g-C_3N_4 equal to 2.19 V vs NHE (at pH 0) that corresponds to the valence band. Considering the band gap value, the conduction band was then located at − 0.44 V vs NHE. These energy levels are different from the ones obtained for the pristine g-C_3N_4 film [1.64 V and − 1.03 V vs NHE (at pH 0) for valence and conduction band, respectively] as a consequence of the influence of boron on the electronic properties of this material. The band gap value and energy levels position of B-doped g-C_3N_4 (1.5 at%) show the great potentiality of this thin film as photoelectrode for CO_2 reduction in PEC technology. LSV were done on these photoelectrodes under AM (air mass) 1.5 solar-simulated light at 100 mW/cm^2 with CO_2-saturated $NaHCO_3$ 0.5 M solution and the results show the production of photocurrents equal to 4 and 6 μA/cm^2 at − 0.4 V vs Ag/AgCl for pristine and doped g-C_3N_4, respectively. Long-time tests were performed and no photocorrosion or reduction phenomena were found for both materials (confirmed by XRD analyses) with ethanol as the main reduction product (78% Faradic efficiency) with a small amount of CO and without the presence of hydrogen. Finally, different co-catalysts were added to the films enhancing the photocurrents and the products generation due to the reduced number of recombination and/or the enhancement of ethanol selectivity produced by multi-electrons mechanisms. Another example of doped g-C_3N_4 is related to the work of Tang et al. (2019) where the influence of Eu(III) as doping agent on the properties of g-C_3N_4 was studied. Eu can work as electrons target to suppress the recombination of photogenerated electrons and holes enhancing the photocatalytic activity. As described before, the high rate of charges recombination is one of the most important issues related to g-C_3N_4. Tang et al. (2019) created photoelectrodes on FTO substrate with pristine or Eu-doped (2, 4, 6, 8, 10 wt%) g-C_3N_4 chemically synthesized. All the samples prepared show a strong characteristic absorption in the range between 400 and 800 nm starting from bare g-C_3N_4 with a band gap energy of 2.65–2.60 eV for the Eu-doped sample (8%). Moreover, through cyclic voltammetry analyses, the active surface area was determined for each sample and the results show the highest value of this parameter for Eu-doped g-C_3N_4. Mott–Schottky analyses on all of the samples prepared showed a n-type semiconductive behavior with europium doping enhancing the charge-carrier concentration. Transient photocurrent was acquired for each sample under 300 W Xe lamp with 0.5 M Na_2SO_4 solution under reduction potential. The higher photocurrent was obtained for the sample doped with 8% of europium (4 μA/cm^2) with respect to the one obtained for the pristine g-C_3N_4 (2.5 μA/cm^2). The main products detected were CH_4 and H_2. The positive effect of Eu-doping was due to the enhanced electrons transfer that finally increases the photocurrent produced. Moreover, the presence of europium improves the charge separation and finally increases the transfer rate of the photogenerated charges. To enhance the photo-electrochemical activity of g-C_3N_4, a nanocomposite with CeO_2 was proposed by Li et al. (2016b). The authors deposited the thin film of pristine g-C_3N_4 and the related nanocomposite with different amount of CeO_2 by electrophoretic process and studied the properties of these photoelectrodes. The band gap energy changed from 2.72 eV for bare g-C_3N_4 to 2.76 eV for the highest amount of CeO_2 passing thorough 2.65 eV with 3% of oxide. All of these materials are, therefore, suitable for solar-drivenapplication. The transient photocurrents were acquired at 0.3 V vs Ag/

AgCl under illumination (300 W Xe lamp) with 0.2 M Na_2SO_4 electrolyte. The obtained photocurrent of nanocomposite was 0.75 µA/cm^2 and this value was higher than the one obtained for the pristine g-C_3N_4 photoelectrode (0.18 µA/cm^2). These differences were due to the highest charge transport for the CeO_2/g-C_3N_4 and to the highly efficient separation and transport of the photogenerated charges enhanced by the redox ability of cerium ($Ce^{3+/4+}$). The main products detected for all samples were CO and CH_4 with the highest amount obtained for the nanocomposite material (only CO was found when bare g-C_3N_4 was used). Liu et al. (2018a) proposed phosphorous-doped g-C_3N_4 nanotubes prepared by thermal reaction starting from g-C_3N_4 nanosheets as efficient material for carbon dioxide photoreduction. As expected, the obtained band gap energy for pristine g-C_3N_4 was 2.70 eV, while the value for the phosphorous-doped sample dropped to 2.58 eV. The doping process induces a red-shift adsorption, hence increasing the portion of light spectrum that can be harvested. Photoelectrodes were prepared on metal substrate by simply drop-casting method and the electrochemical and photo-electrochemical properties were determined with 300 W Xe lamp with 0.5 M Na_2SO_4 electrolyte. The Mott–Schottky analyses showed for phosphorous-doped g-C_3N_4 nanotubes and pristine g-C_3N_4 n-type conductivity; while the valence band and conduction band were found 1.80 and 1.75 and -0.90 and -1.07 V vs NHE, respectively. These results indicate that both materials tested possess suitable thermodynamic energy for carbon dioxide and hydrogen reduction reactions. Phosphorous-doped g-C_3N_4 nanotubes show higher photocurrent (30 µA/cm^2) than the pristine g-C_3N_4 (15 µA/cm^2). The electrochemical impedance analyses (EIS) show that the phosphorous doping increases not only the optical absorption but also the charge separation and surface charge transfer. The main product obtained from carbon dioxide reduction was found to be CH_4 derived from CO. At the same time also H_2 was detected.

3 Electrocatalytic CO_2 reduction (CO_2RR)

Electroreduction represents a valuable and highly investigated approach for CO_2 conversion into products of added value. The CO_2 molecule is extremely stable, which makes its electrochemical conversion into target chemicals rather difficult. As a result, relatively high overpotentials are generally required to accomplish the first CO_2RR step, this latter being commonly recognized as the rate-determining step that involves the re-arrangement of a linear CO_2 molecule to a bent radical anion $CO_2^{\cdot-}$ (Duan et al. 2017). Beyond large research efforts devoted to metal-based catalysts, recent years have boosted metal-free heterodoped carbon-based nanomaterials as alternative, sustainable and highly efficient catalytic systems to promote CO_2RR (Genovese et al. 2018; Duan et al. 2017; Liu et al. 2017b; Zheng et al. 2017). While plain C-based materials display only negligible CO_2RR, the inclusion of heteroatoms in their honeycomb structure with the subsequent alteration of their pristine electroneutrality has unveiled a rich and to some extent unexpected electrocatalytic activity towards CO_2 reduction. Both electronic and morphological properties of C-nanomaterials change with the doping using heteroatoms forming high-energy surface sites suitable for CO_2 activation (Chai and Guo 2016).

Due to the multiple-electrons nature of CO_2RR, the process potentially leads to different C1 and/or C2 products (see also Table 1). The control on the nature of CO_2 reduction products necessarily passes through the comprehension of the structure/reactivity relationships of carbon-based materials in the process. Unfortunately, due to the structural and chemico/physical complexity of hetero-doped materials, it appears rather difficult to get unambiguous evidences on the nature of the active sites directly engaged in the transformation. For instance, the structural complexity of N-doped carbon-based catalysts, where different N-configurations coexist at the same time, hamper a clear-cut comprehension of the nature of active sites responsible of the observed electrocatalytic CO_2RR performance. The join combination of experimental outcomes and DFT calculations has been exerted by several research teams with the aim to shed light on this matter often coming to controversial conclusions. Several authors have claimed pyridinic nitrogen sites as the N-configuration of choice for the process to occur due to the basic properties of pyridinic sites capable to foster CO_2 coordination. On the other hand, other reports indicate either quaternary nitrogens or N-neighboring carbon atoms as the positively charged sites for the stabilization of the $CO_2^{\cdot-}$ radical anion coming from the first kinetically sluggish electron-transfer process.

It is evident that further research efforts are still necessary to enlarge the knowledge on this matter before getting a mature catalyst technology opened to the rational design of carbon-based metal-free electrocatalysts and featured by high performance and controlled selectivity.

3.1 Reaction environment: the choice of the electrolyte

The first contribution on the use of carbon-based metal-free electrocatalysts for CO_2RR was reported by Kumar et al. (2013). In their seminal work, authors demonstrated the ability of N-doped carbon nanofibers to promote the selective CO_2 reduction to CO with a Faradaic efficiency (FE) up to 98%. The reactions were carried out in an ionic liquid (IL) (EMIM-BF_4) whose ability to actively participate into the process through the formation of an EMIM-CO_2

intermediate was considered as the driving-force fostering CO_2 reduction to CO. Even if the reaction mechanism could not be elucidated due to the complexity of the N-doped material, high-resolution XPS analyses on the material before and after catalysis led authors to identify C atoms adjacent to pyridinic sites as the active species engaged into the process. More recently, Sun et al. (2016) prepared a N-doped carbon graphene-like material capable to produce methane (CH_4) using ILs as electrolyte. Authors obtained CH_4 with extremely high FE (93.5%) pointing out pyridinic and pyrrole/pyridonic groups as the active sites for the process, while stressing the importance in the use of ILs for driving the process towards methane as reaction target. This work represents the first and to date the unique example of a metal-free material for the CO_2 selective electroreduction to methane. Besides ILs as electrolytes, the only other non-aqueous reaction medium explored in the process was based on methanol (MeOH). Nakata and Einaga's group developed boron-doped nanodiamonds (B-NDs) capable of promoting CO_2RR in MeOH giving formaldehyde as the major product with a Faradic efficiency up to 74% (Nakata et al. 2014). The choice of MeOH as electrolyte was due to the high solubility of CO_2 (up to five times higher than in water) that obviously fosters the reduction process.

Since these contributions, other examples of doped carbon-based materials have been developed and applied to CO_2RR by giving increased attention to the choice of the reaction environment. In particular, the use of more benign aqueous electrolytes has been addressed to make the process more sustainable, cheap and feasible for future and large-scale applications. Despite of several advantages coming from of the use of an aqueous medium, other critical issues still remain to be properly addressed and overcome as to render this chemical environment really convenient from an electrochemical view-point. Indeed, CO_2 shows only a moderate solubility in water and CO_2RR in aqueous media occurs at higher overpotentials, thus making the side hydrogen evolution reaction (HER) a highly competitive process. As a result, Faradaic efficiency (FE) for CO_2RR and catalyst productivity can be significantly affected, thus resulting in moderate electrocatalytic performance. It is, therefore, mandatory to design catalysts able to reduce CO_2 efficiently already at relatively low potential values, to minimize as much as possible the occurrence of HER. The first example of CO_2RR conducted in aqueous medium ($KHCO_3$ solution) has been reported by Zhang et al. (2014). They prepared N-doped carbon nanotubes coated with a thin polyethyleneimine (PEI) film as highly selective electrocatalysts for formate production. The combination of N-CNTs with the polymer was found to reduce markedly the overpotential value at which CO_2RR starts (200 mV less respect to plain N-CNTs), thus enhancing FE to formate up to 87% with a current density value of 9.5 mA/cm^2. The PEI overlayer was supposed to play a double role: (1) concentrate CO_2 at the electrode surface and (2) stabilize the $CO_2^{\cdot-}$ radical anion, the latter being again the presumed intermediate formed after the first rate-determining electron transfer. Authors' conclusion was that the basic character of PEI-coated N-CNTs was mandatory to ensure a relatively high CO_2 concentration at the catalyst surface, a key pre-requisite for the CO_2RR process to occur efficiently.

Among aqueous electrolytes, bicarbonate solutions are the most commonly used for running CO_2RR. However, its use has raised several remarks regarding its effective role in the process. Indeed, bicarbonate can be considered itself as a CO_2 source through the carbon dioxide–bicarbonate equilibrium. Liu et al. (2015) observed the dependence of CO_2 reduction rate on HCO_3^- concentration, with current density increasing linearly with the solution molarity. More recently, Hursán and Janáky (2018) have demonstrated by means of isotopically labelled $^{13}CO_2$ and $H^{13}CO_3^-$ that bicarbonate does not directly contribute to the generation of CO_2RR products but it rather behaves as a CO_2 reserve by regularly supplying $CO_{2(aq)}$ dissolved at the electrode surface.

3.2 Hetero-doped (N, S, B) C-nanomaterials in CO_2RR

3.2.1 The 2 electrons reduction process to carbon monoxide (CO)

Carbon monoxide (CO) represents the most commonly observed reduction product with carbon-based CO_2RR electrocatalysts. Besides the above-mentioned contribution by Kumar et al. (2013) where N-doped carbon nanofibers were used to promote the CO_2RR to CO in IL with high Faradaic efficiency (98%), many other N-doped materials have been prepared and successfully applied to the selective carbon monoxide production. Wu et al. (2015) and Sharma et al. (2015) prepared N-doped carbon nanotubes (N-CNTs) by chemical vapor deposition (CVD) with interesting electrocatalytic activity in the CO production using an aqueous bicarbonate solution as electrolyte, with a maximum Faradaic efficiency of 80% already at low potential values (− 0.78 V vs. SHE). The combination of experimental results with XPS analyses and DFT calculations led the authors to identify both N-pyridinic and N-graphitic (quaternary) as the active sites for the CO_2 activation. On the other hand, pyrrolic groups were supposed to have no impact on CO_2RR. Later, Xu et al. (2016) synthesized N-CNTs by calcination of a mixture of poly(diallyldimethylammonium chloride) and oxidized CNTs to be tested as CO_2RR electrocatalysts. CO was found to be the main reaction product with FE up to 90%. DFT calculation recognized quaternary nitrogen sites as the main players for the observed activity due to their ability to stabilize $CO_2^{\cdot-}$ intermediate by reducing the free energy associated with the first electron-transfer process. Other than monodimensional (1D) N-CNT systems, several 2D and 3D N-doped composites have been developed and exploited in the process. Lu et al. (2016) prepared a graphitic carbon nitride (g-C_3N_4)/MWCNTs composite by means of a high-temperature polycondensation of dicyandiamide with oxidized CNTs. Authors attributed the catalyst ability to selectively reduce CO_2 to CO (FE = 60%) to a synergistic effect between carbon nitride and MWCNTs. In particular, they invoked the formation of active carbon–nitrogen bonds along with the high specific surface area and material conductivity as the key factors for the observed catalytic outcomes. An impressive CO_2RR activity was reported later by Jhong et al. (2017) that prepared a g-C_3N_4/MWCNTs composite by depositing a thin layer of nitride on a pure MWCNTs surface. With FE as high as 98% in the CO_2RR to CO and a maximum current density of 90 mA/cm^2, this composite material ranks among the most efficient metal-free carbon-based catalysts for carbon monoxide production reported so far. Most recently, a 2D ultrathin g-C_3N_4 layer has been developed by a hydrothermal–thermal exfoliation method and reported to boost CO_2RR to CO as the main product (FE = 80%) (Zhang et al. 2018b). The polarized surface induced by the ultrathin nanostructure was claimed by authors to play a key role in enhancing CO_2RR activity. Looking finally at three-dimensional carbon materials, 3D hierarchical porous N-doped carbons prepared by pyrolysis of biomasses (Li et al. 2017a) and 3D graphene foam grown by CVD on a template (Wu et al. 2016a) have been reported for the selective CO_2RR to CO with comparable selectivity (FE = 85%). In both cases, authors have claimed pyridinic nitrogen defects as essential for the CO_2 activation and conversion to CO.

From the literature overview outlined above, it is clear that the debate on the structure/composition/reactivity relationship at the origin of the catalytic performance of these metal-free systems in CO_2RR is still open. Despite many research efforts both on experimental and theoretical ground, the structural complexity of doped nanocarbons along with their variable N-composition (coexistence of different N-configurations as a function of the material synthesis) hampers the unambiguous identification of CO_2RR active sites. On this ground, a rational bottom–up synthesis based on the exohedral chemical functionalization of plain C-nanomaterials with defined N-containing functionalities has been recently developed by some of us (Tuci et al. 2018). Such a non-conventional approach to the N-decoration of carbon nanostructures has allowed a fine-tuning of N-containing functional groups at the nanomaterial outer surface, thus offering unique hints to the comprehension of their role in the underlying CO_2RR mechanism. In particular, basic NH-aziridine groups have been proven to promote the selective CO_2 reduction to CO with markedly higher performance compared to that of classic pyridine groups (often claimed in the literature as the active species for the process). The higher activity of the former is basically ascribed to their inherent ability to chemisorb CO_2 through the formal aziridine-carbonation reaction. Such an effect is claimed to drive the catalytic process by changing CO_2 geometry from linear to bent (in the carbonation product) and thus favoring the kinetically sluggish first electron transfer process for the generation of the $CO_2^{\cdot-}$ species. Finally, the latter is stabilized by the positively charged carbon atoms neighboring the N site before undergoing a further 1 electron reduction step with the participation of two H^+ (Fig. 6).

Beyond nitrogen as dopant, just a few examples of carbon nanomaterials doped with other heteroatoms have been reported so far for promoting CO_2RR to CO. Sulfur was chosen as a carbon dopant with very modest result. Indeed, only 2% of FE towards CO was found with S-doped nanoporous carbon; whereas, a slight increase (up to 11%) was reported for N and S co-doped materials at work in the process (Li et al. 2016b). Better results have been achieved with F- and P-doped materials. As for the former, a F-doped sample was obtained by a simple pyrolysis of a commercial carbon with PTFE as the fluorine source (Xie et al. 2018). The catalyst exhibited high FE to CO (up to 90%) with the positive charged carbon atoms identified by authors as the active sites for the process. Indeed, due to the high electronegativity of fluorine nuclei, a relevant positive charge density on the neighboring carbon atoms was supposed to strongly bind the CO_2 reduction intermediates, ultimately favoring CO_2RR and suppressing the competitive HER. Finally phosphorous, as a heteroatom possessing the same valence electrons as nitrogen, was explored as dopant in C-nanostructures. On this ground, P-doped onion-like carbons have been reported by Liu et al. (2018b) as efficient catalysts for CO_2 reduction to CO with FE up to 81%. Authors point out P–C functionalities as more active than P–O ones in stabilizing CO_2 reduction intermediates and in enhancing the electronic transfer. Overall, P-doped carbons demonstrate to be valuable alternatives to N-doped nanocarbons offering comparable performance for CO production.

3.2.2 The 2 electrons reduction process to formate (HCO_2^-) and formaldehyde (HCOH)

Formate (HCO_2^-) represents an important 2 electrons reduction product of CO_2. Beyond the above-mentioned paper by the Zhang et al. (2014), there are just a few examples of N-doped nanocarbons employed in the CO_2RR to give formate as the main reduction product. Wang et al. (2016) and Wang et al. (2017) have described the use of N-doped graphene and N-doped nanoporous carbons/carbon-nanotube composite membranes for the CO_2RR to HCO_2^- with FE up to 73 and 81%, respectively. Both

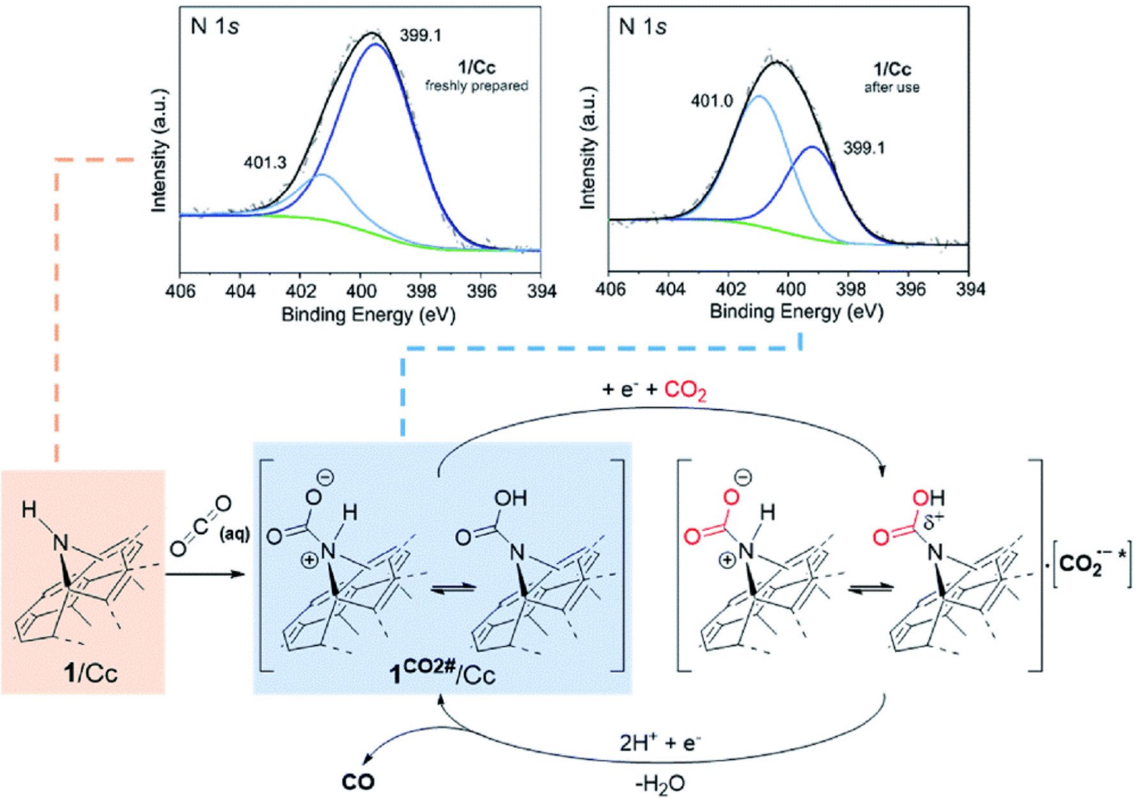

Fig. 6 CO_2 electroreduction process via CO_2(aq) chemisorption to NH-aziridine groups (amine carbonation). N 1s core regions and relative fits for the high-resolution XPS spectrum of catalyst before (left) and after (right) the electrocatalytic run are shown in the upper part of the scheme. N 1s components at higher binding energies (401.3 and 401.0 eV) are attributed to the formation of amine carbonate whereas components at 399.1 eV belong to free aziridine groups. Reproduced from Tuci et al. (2018) by permission of The Royal Society of Chemistry

papers agree on the central role played by carbon atoms neighboring pyridinic sites for the CO_2 coordination without any direct involvement of N atoms. Even if authors did not give an explanation on why their N-doped systems produce formate instead of the most common CO obtained with similar materials (see Sect. 3.2.1), they invoke a reaction mechanism where CO_2 coordinates to the catalyst (and in particular to the carbon atom adjacent to N-pyridine) through one of its oxygen atoms (Fig. 7).

This reactivity accounts for a radically different coordination mode of CO_2 respect to that postulated for N-doped nanocarbons engaged in the CO_2RR to CO, where the substrate (CO_2) was supposed to interact with the catalyst through its carbon atom (see Sect. 3.2.1 and Fig. 6) (Sharma et al. 2015; Tuci et al. 2018; Li et al. 2016a). Therefore, the different CO_2 coordination mode can be invoked as a key factor to control the process selectivity towards CO or formate. This hypothesis would also explain CO_2RR performance observed with differently doped systems, such as with B-doped carbon nanomaterials, where the electron-poor nature of the heterodopants

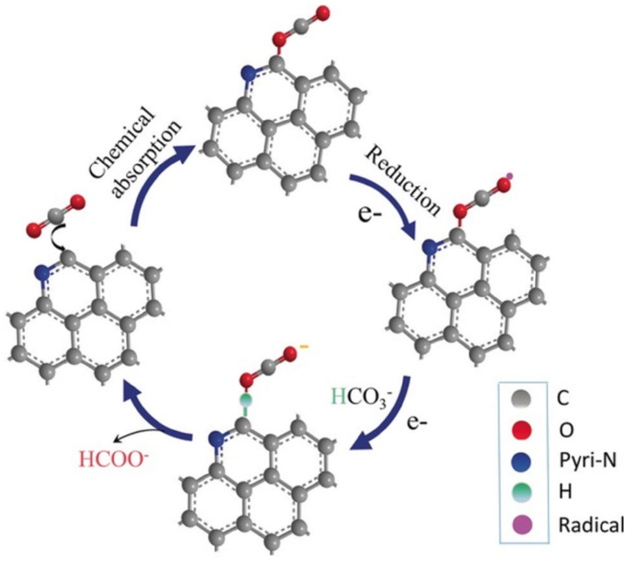

Fig. 7 Proposed mechanism of the CO_2RR in 0.1 M $KHCO_3$ aqueous solution by HNCM/CNT membrane. Reproduced from Wang et al. (2017) with permission from Wiley–VCH

is supposed to foster its coordination with one of the more electron-rich oxygen atoms of CO_2.

To date, only a few examples of B-doped nanocarbons have been exploited for CO_2 electroreduction. Among them, B-doped graphene prepared by pyrolysis of GO with boric acid has been reported to produce HCO_2^- with a FE of 66% (Sreekanth et al. 2015). Two research groups have independently demonstrated that B-doped nanodiamonds (B-NDs) were electrocatalytically active materials for CO_2RR to formaldehyde and formate (main by-product) with FEs of 74 and 26% or 54% and 14%, respectively (Nakata et al. 2014; Liu et al. 2017b). Taking into account that formaldehyde (HCOH) derives directly from the formate reduction (Nakata et al. 2014), it is evident that B-doped samples foster the HCO_2^- conversion once again through the coordination of its oxygen atom to the electron-poor B-sites. To the best of our knowledge, B-doped nanodiamonds are unique materials for the CO_2RR to HCOH, thus unveiling that B-doping of sp^3 hybridized nanocarbons are somehow suitable systems for promoting the further HCO_2^- reduction to formaldehyde (Nakata et al. 2014). On the other hand, there are no examples of N-doped nanocarbons reported to date as active electrocatalysts for the generation of HCOH as the main species.

Therefore, it can be inferred that the distinctive behavior of B-doped C-nanomaterials in CO_2RR mirrors with the different coordination mode of the substrate (CO_2) at the catalyst active sites. Boron is an electron-poor element respect to carbon and it prefers coordination to one oxygen atom of CO_2. On the other hand, the electron-rich N sites in N-doped C-nanocarbons will bind CO_2 through its carbon atom, preferentially. Even if any definitive conclusion on the underpinning CO_2RR mechanism is formally hampered by the complexity of the electrocatalytic materials, it seems reasonable to postulate that different coordination modes of CO_2 are responsible of the observed process selectivity towards CO or formate.

3.2.3 CO_2RR to C2 products

An important class of CO_2 reduction products is represented by C2 compounds such as acetate (CH_3COO^-), ethanol (CH_3CH_2OH) or light hydrocarbons. C2 products are obviously highly attractive targets although their selective synthesis from CO_2 remains rather difficult to be addressed because the process requires C–C coupling step in addition to the classical CO_2 reduction process. The following sections summarize the literature achievements in this challenging research area.

3.2.3.1 CO_2RR to acetate ions The first example of a C2 compound synthesized by electrochemical CO_2 reduction has been reported by Liu et al. (2015). They designed a N-doped nanodiamond/Si rod array enabling CO_2 conversion to acetate (FE = 77.6%) together with a minor amount of formate (FE = 14.6%). Although further studies are needed to better understand the origin of acetate selectivity in the process, authors postulated that N-Csp^3 functionalities in N-NDs make the kinetic for a new C–C bond formation faster than that of the protonation of the $CO_2^{\cdot-}$ intermediate to give formate. Two years later, the same group reported on analogous N-NDs for acetate production with a FE of 62% (Liu et al. 2017a). Interestingly, these authors also demonstrated the radically different behavior of the boron-doped counterparts (B-NDs). Indeed, the latter allowed CO_2 reduction to C1 products only (i.e., formaldehyde and formate, see also Sect. 3.2.2). Accordingly, they inferred that N doping in NDs was somehow responsible for the occurrence of C–C coupling in the process, thus paving the way to the direct CO_2 electrochemical conversion to C2 compounds.

3.2.3.2 CO_2RR to ethanol One of the more desired CO_2 reduction products is represented by ethanol, an important raw material and a promising renewable fuel. To date, the highest FE towards EtOH (93.2%) has been reported by Liu et al. (2017b) with B–N co-doped NDs. Their material has been found to efficiently promote the C–C coupling to EtOH, while limiting both C1 products formation and HER. With the support of DFT calculations, authors demonstrated that their catalyst superior performance for EtOH production originates from the synergistic effect of B–N co-doping that promote the coupling of two neighboring CO* species to give C2 products. Their conclusions confirm once again the supposed pivotal role of N-doping in NDs for promoting the C–C coupling (see Sect. 3.2.3.1).

In the same period, metal-free cylindrical mesoporous N-doped carbons (c-NC) synthesized by Song et al. (2017) using a soft-template method have been proven to convert CO_2 into ethanol with FE as high as 77% at low potential values (0.56 V vs. RHE). Noteworthy, the only by-product observed is represented by H_2 due to HER, with no other reduction products coming from CO_2. Again, the key feature for the selective production of ethanol lies on the occurrence of a C–C coupling, while limiting the competitive CO and/or other C1 products formation. Authors have assumed that pyridinic nitrogens are the preferential activation sites for CO_2 to give CO* intermediates stabilized by the material electron-rich cylindrical surface, which supplies the electrons for CO* dimerization to ethanol while avoiding the undesired release of CO as reduction product. To demonstrate the superiority of such a cylindrical mesoporous structure, the inverse mesoporous N-doped carbon (denoted as i-NC) that preserves similar pore parameters and N-content, was also prepared for comparison (Fig. 8). Over i-NC, the maximum ethanol FE reached only 44% with formation also of CO and H_2 as by-products.

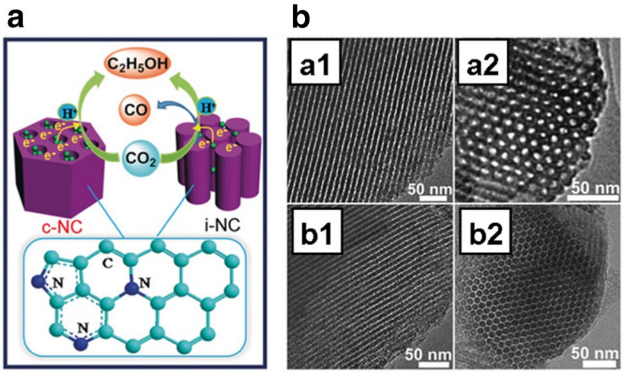

Fig. 8 **A** Illustration of c-NC and i-NC for CO_2 electroreduction. **B** TEM images of (**a1**, **a2**) c-NC and (**b1**, **b2**) i-NC viewed along (**a1**, **b1**) [110] and (**a2**, **b2**) [100] directions. Reproduced from Song et al. (2017) with permission from Wiley–VCH

3.2.3.3 CO_2RR to light hydrocarbons Besides methane (CH_4) as the simplest hydrocarbon prepared from CO_2RR in 2016 (see Sect. 3.1) (Sun et al. 2016), only one example of C2 hydrocarbon has been reported to date with appreciable FE values. Wu et al. (2016b) have demonstrated that N-doped graphene quantum dots (NGQDs) electrocatalysts lead to ethylene (C_2H_6) as the major CO_2RR product, although with moderately low FE (31%). Indeed, products distribution appears relatively broad with the formation of EtOH and acetate other than C1 products (CO and formate) and C3 compounds such as *n*-propanol. The authors indicate, among the various N-configurations available in their material, N-pyridinic as the most active site for the process to occur. In particular, they postulated N-pyridinic edge sites as those engaged in the new C–C bond formation. As a result, the higher the amount of pyridinic edge sites in NGQDs, the higher the yield of C2 products.

4 Conclusions

This review aims at describing the state-of-the-art carbon-based nanomaterials as metal-free catalysts for CO_2 photoelectrochemical (PEC) and electrochemical reduction (CO_2RR). Despite a certain number of interesting reports appeared in the literature up to date, one of the main issues still pending within these reduction technologies deals with the development of efficient and robust catalytic materials capable to operate under aqueous environments for the highly selective CO_2 reduction to molecules of added value with high productivity while limiting the occurrence of side reactions (i.e., HER).

Conducting polymers and g-C_3N_4 represent attractive materials for PEC applications due to their low cost, abundance and low toxicity. However, some issues such as low photocurrent, charges recombination and films inhomogeneity need to be overcome to get highly efficient materials for CO_2 activation and conversion. For example, to reduce the production costs and increase the sustainability of the overall process, additive manufacturing technology should be applied while producing organic photoelectrodes. The development and optimization of these processes also passes through the use of ink-jet or spray-coating preparation methods. Doping processes and low-cost polymerization methods (such as electropolymerization) should be used for the realization of highly efficient and stable photoelectrodes; while PPy and PEDOT should be considered in more details also for carbon dioxide conversion. In fact, PEDOT possesses a higher potentiality for carbon dioxide reduction by PEC technology due to the presence of sulfur atoms on its polymeric chain. The main limitations on the application of g-C_3N_4 are the fast recombination of the photogenerated charges and poor electronic conductivity as well as the limited absorption of visible light. These issues can be overcome building highly conductive nanohybrid materials with a metallic nanoparticles coating without reducing the band gap energy of g-C_3N_4. At the same time, the lower photocurrent produced should be improved by doping processes, realization of new interfaces and using a co-catalyst material. Also the deposition process is crucial and a new technique should be created for the film deposition directly on the conducting substrate.

As for CO_2RR, one main issue is represented by selectivity towards a target product and on this ground, some general trends can be summarized on the basis of the most recent litterature outcomes. CO is the most common reduction product when hetero-elements such as N, P or F are used as dopants in C-based nanostructures. On the other hand, when the electropositive B atom is introduced in the C-network, formate represents the preferred 2-electrons reduction product. No B-doped nanocarbons have been reported to date as suitable electrocatalysts for CO_2RR to CO, while formaldehyde has been observed as the main CO_2RR product with B-doped nanodiamonds as electrocatalysts only, unveiling the pivotal role played by the B/C-sp^3 combination to give HCOH selectively. No carbon-based metal-free catalysts have been reported to date for methanol synthesis with appreciable FEs, while methane has been obtained with N-doped nanocarbons only conducting CO_2RR in IL electrolytes that are supposed to play a non-trivial role in driving selectivity towards CH_4.

C2 compounds are certainly the more attractive reduction products in CO_2RR, although just a few examples of metal-free catalysts have been reported to date to foster the transformation efficiently. Even if the reaction mechanism is still far from being fully explained, one of the main challenges to be addressed to obtain C2 products is to prepare electrocatalytic materials featuring an ideal binding strength towards CO_2 reduction intermediates and products. Taking into account CO as the most common 2 electrons reduction product, electrocatalysts that bind CO weakly will produce it as the major product because it quickly moves away for the catalyst active sites. On the other hand, catalysts that bind CO too strongly will result in poor catalytic activity due to poisoning effects; this is not usually encountered with metal-free carbon-based materials but it is a well-known problem encountered with noble metal-based electrocatalysts (e.g., Pt). The key point is, therefore, to bind CO with the "just right" strength to avoid its fast release from active sites and allow its further evolution into C2 compounds. This key issue has to be accomplished with a tricky combination of selected dopant species and tailored chemico-physical/morphological properties of nanocarbon materials. It is evident that additional research efforts are needed for the rational design of robust and efficient catalysts with targeted selectivity towards a desired product. To this aim, one main step forward is represented by a deep comprehension of the mechanisms at work in the CO_2RR along with the elucidation of the structure/composition/reactivity relationships between doped nanocarbons and CO_2. A rational bottom–up synthesis of hetero-doped carbon nanomaterials combined with DFT calculations can give an important boost to get new progresses in the field and to accomplish many of the ambitious goals of this technology.

Acknowledgements G.T and G.G. thank the TRAINER project (Catalysts for Transition to Renewable Energy Future) of the "Make our Planet Great Again" program, Agence Nationale de la Recherche (Ref. ANR-17-MPGA-0017) and the Italian MIUR (Ministero dell'Istruzione dell'Università e della Ricerca) through the PRIN 2015 Project SMARTNESS (2015K7FZLH) "Solar driven chemistry: new materials for photo- and electrocatalysis" for financial support. All authors also acknowledge DSCTM-CNR for support to the preparation of this contribution.

Compliance with ethical standards

Conflict of interest The authors declare that they have no conflict of interest.

References

(2019) Carbon-based metal-free catalysts. Adv Mater 31:1970090. https://doi.org/10.1002/adma.201970090

Armaroli N, Balzani V (2016) Solar electricity and solar fuels: status and perspectives in the contest of the energy transition. Chem Eur J 22:32–57

Azofora LM, McFarlane DR, Sun C (2016) A DFT study of planar vs. corrugated graphene-like carbon nitride ($g\text{-}C_3N_4$) and its role in the catalytic performance of CO_2 conversion. Phys Chem Chem Phys 18:18507–18514

Beladed C, Rekhila G, Doulache M, Zitouni B, Trari M (2013) Photo-electrochemical characterization of polypyrrole: application to visible light induced hydrogen production. Sol Energy Mater Sol Cells 114:199–204

Cao S, Li Y, Zhu B, Jaroniec M, Yu J (2017) Facet effect of Pd cocatalyst on photo-catalytic CO_2 reduction over $g\text{-}C_3N_4$. J Catal 349:208–217

Chai G-L, Guo Z-X (2016) Highly effective sites and selectivity of nitrogen-doped graphene/CNT catalysts for CO_2 electrochemical reduction. Chem Sci 7:1268–1275

Chang X, Wang T, Gong J (2016) CO_2 photo-reduction: insights into CO_2 activation and reaction on surface photocatalysis. Energy Environ Sci 9:2177–2196

Cui H, Guo Y, Guo L, Wang L, Zhou Z, Peng Z (2018) Heteroatom-doped carbon materials and their composites as electrocatalysts for CO_2 reduction. J Mater Chem A 6:18782–18793

Dai L (2004) Intelligent macromolecules for smart devices. Conducting polymers, 1st edn. Springer, London, pp 42–80

Dong YM, Chen YM, Jiang PP, Wang GL, Wu XM, Wu RX (2016) A novel $g\text{-}C_3N_4$ based photocathode for photoelectrochemical hydrogen evolution. RCS Adv 6:7465–7473

Duan X, Xu J, Wei Z, Ma J, Guo S, Wang S, Liu H, Dou S (2017) Metal-free carbon materials for CO_2 electrochemical reduction. Adv Mater 29:1701784–1701804

Fan W, Chen C, Bai H, Luo B, Shen H, Shi W (2016) Photosensitive polymer and semiconductor bridged by Au plasmon for photoelectrochemical water splitting. Appl Catal B Environ 195:9–15

Fang Y, Wang X (2018) Photocatalytic CO_2 conversion by polymeric carbon nitride. Chem Commun 54:5674–5687

Fang Y, Li X, Wang X (2018a) Synthesis of polymeric carbon nitride films with adhesive interfaces for solar water splitting devices. ACS Catal 8:8774–8780

Fang YF, Xu Y, Li X, Ma Y, Wang X (2018b) Coating polymeric carbon nitride photoanodes on conductive Y:ZnO nanorods arrays for overall water splitting. Angew Chem Int Ed 57:9749–9753

Genovese C, Schuster ME, Gibson EK et al (2018) Operando spectroscopy study of the carbon dioxide electro-reduction by iron species on nitrogen-doped carbon. Nat Commun 9:935–947. https://doi.org/10.1038/s41467-018-03138-7

Ghosh S, Mallik AK, Basu RN (2018) Enhanced photocatalytic activity and photoresponse of poly(3,4-ethylenedioxythiophene) nanofibers decorated with gold nanoparticle under visible light. Sol Energy 159:548–560

Goettmann F, Thomas A, Antonietti M (2007) Metal-free activation of CO_2 by mesoporous graphitic carbon nitride. Angew Chem Int Ed 46:2717–2720

Hursán D, Janáky C (2018) electrochemical reduction of carbon dioxide on nitrogen-doped carbons: insights from isotopic labeling studies. ACS Energy Lett 3:722–723

Hursán D, Kormányos A, Rajeshwar K, Janáky C (2016) Polyaniline films photoelectrochemically reduce CO_2 to alcohols. Chem Commun 52:8858–8861

Jhong H-RM, Tornow CE, Smid B, Gewirth AA, Lyth SM, Kenis PJA (2017) A nitrogen-doped carbon catalyst for electrochemical CO_2 conversion to CO with high selectivity and current density. Chemsuschem 10:1094–1099

Joy J, Mathew J, George SC (2018) Nanomaterials for photoelectrochemical water splitting—review. Int J Hydrogen Energy 43:4804–4817

Kalamaras E, Maroto-Valer MM, Shao M, Xuan J, Wang H (2018) Solar carbon fuel via photoelectrochemistry. Catal Today 317:56–75

Kao E, Liang Q, Bertholet GR-K, Zang X, Park HS, Bae J, Lu J, Lin L (2018) Electropolymerized polythiophene photoelectrodes for photocatalytic water splitting and hydrogen production. Sensors Actuators A Phys 277:18–25

Kormányos A, Ondok R, Janáky C (2017) Electrosynthesis and photoelectrochemical properties of polyaniline/SiC nanohybrid electrodes. Electrochim Acta 256:73–80

Kumar B, Asadi M, Pisasale D, Sinha-Ray S, Rosen BA, Haasch R, Abiade J, Yarin AL, Salehi-Khojin A (2013) Renewable and metal-free carbon nanofibre catalysts for carbon dioxide reduction. Nat Commun 4:2819–2827

Li W, Bandosz TJ (2018) Role of heteroatoms in S–N-codoped nanoporous carbon materials in CO_2 (photo)electrochemical reduction. Chemsuschem 11:2987–2999

Li M, Zhang L, Wu M, Du Y, Fan X, Wang M, Zhang L, Kong Q, Shi J (2016a) Mesostructured CeO_2/g-C_3N_4 nanocomposites: remarkably enhanced photocatalytic activity for CO_2 reduction by mutual component activations. Nano Energy 19:145–155

Li W, Seredych M, Rodriguez-Castellun E, Bandosz TJ (2016b) Metal-free nanoporous carbon as a catalyst for electrochemical reduction of CO_2 to CO and CH_4. Chemsuschem 9:606–616

Li W, Herkt B, Seredych M, Bandosz TJ (2017a) Pyridinic-N gropus and ultramicropore nanoreactors enhance CO_2 electrochemical reduction on porous carbon catalysts. Appl Catal B Environ 207:195–206

Li F, Xue M, Knowles GP, Chen L, MacFarlane DR, Zhang J (2017b) Porous nitrogen-doped carbon derived from biomass for electrocatalytic reduction of CO_2 to CO. Electrochim Acta 245:561–568

Liu Y, Chen S, Quan X, Yu H (2015) Efficient electrochemical reduction of carbon dioxide to acetate on nitrogen-doped nanodiamond. J Am Chem Soc 137:11631–11636

Liu TF, Ali S, Lian Z, Li B, Su DS (2017a) CO_2 electoreduction reaction on heteroatom doped carbon cathode materials. J Mater Chem A 5:21596–21603

Liu Y, Zhang Y, Cheng K, Quan X, Fan X, Su Y, Chen S, Zhao H, Zhang Y, Yu H, Hoffmann MR (2017b) Selective electrochemical reduction of carbon dioxide to ethanol on a boron- and nitrogen-Co-doped nanodiamond. Angew Chem Int Ed 56:15607–15611

Liu B, Ye L, Wang R, Yang J, Zhang Y, Guan R, Tian L, Chen X (2018a) Phosphorus-doped graphitic carbon nitride nanotubes with amino-rich surface for efficient CO_2 capture, enhanced photocatalytic activity, and product selectivity. ACS Appl Mater Interfaces 10:4001–4009

Liu TF, Ali S, Lian Z, Si CW, Su DS, Li B (2018b) Phosphorus-doped onion-like carbon for CO_2 electrochemical reduction: the decisive role of the bonding configuration of phosphorus. J Mater Chem A 6:19998–20004

Lu X, Tan TH, Ng YH, Amal R (2016) Highly selective and stable reduction of CO_2 to CO by a graphitic carbon nitride/carbon nanotube composite electrocatalyst. Chem Eur J 2:11991–11996

Lu L, Lv Z, Si Y, Liu M, Zhang S (2018) Recent progress on band and surface engineering of graphitic carbon nitride for artificial photosynthesis. Appl Surf Sci 462:693–712

Ma XZ, Zhang JT, Wang B, Li QG, Chu S (2018) Hierarchical Cu_2O foam/g-C_3N_4 photocathode for photoelectrochemical hydrogen production. Appl Surf Sci 427:907–916

Nakata K, Ozaki T, Terashima C, Fujishima A, Einaga Y (2014) High-yield electrochemical production of formaldehyde from CO_2 and seawater. Angew Chem Int Ed 53:871–874

Ponnurangam S, Chernyshova IV, Somasundaran P (2017) Nitrogen-containing polymers as a platform for CO_2 electroreduction. Adv Colloid Interface Sci 244:184–198

Remiro-Buenamañana S, García H (2019) Photoassisted CO_2 conversion to fuels. ChemCatChem 11:342–356

Sangiorgi N, Sanson A (2017) Influence of electropolymerized polypyrrole optical properties on bifacial dye-sensitized solar cells. Polymer 125:208–216

Sangiorgi N, Sangiorgi A, Tarterini F, Sanson A (2019) Molecularly imprinted polypyrrole counter electrode for gel-state dye-sensitized solar cells. Electrochim Acta 305:322–328

Saraga N, Kamimura S, Tsubota T, Ohno T (2016) Photoelectrochemical CO_2 reduction by a p-type boron-doped g-C_3N_4 electrode under visible light. Appl Catal B Environ 192:193–198

Sharma PP, Wu J, Yadav RM, Liu M, Wright CJ, Tiwary CS, Yakobson BI, Lou J, Ajayan PM, Zhou X-D (2015) Nitrogen-doped carbon nanotube arrays for high-efficiency electrochemical reduction of CO_2: on the understanding of defects, defect density, and selectivity. Angew Chem Int Ed 54:13701–13705

Shen M, Zhang L, Shi J (2018) Converting CO_2 into fuels by graphitic carbon nitride-based photocatalysts. Nanotechnology 29:412001–412013

Smith RDL, Pickup PG (2010) Nitrogen-rich polymers for the electrocatalytic reduction of CO_2. Electrochem Commun 12:1749–1751

Song Y, Chen W, Zhao C, Li S, Wei W, Sun Y (2017) Metal-free nitrogen-doped mesoporous carbon for electroreduction of CO_2 to ethanol. Angew Chem Int Ed 56:10840–10844

Sreekanth N, Nazrulla MA, Vineesh TV, Sailaja K, Phani KL (2015) Metal-free boron-doped graphene for selective electroreduction of carbon dioxide to formic acid/formate. Chem Commun 51:16061–16064

Sun X, Kang X, Zhu Q, Ma J, Yang G, Liu Z, Han B (2016) Very highly efficient reduction of CO_2 to CH_4 using metal-free N-doped carbon electrodes. Chem Sci 7:2883–2887

Sun Z, Wang H, Wu Z, Wang L (2018) g-C_3N_4 based composite photocatalysts for photocatalytic CO_2 reduction. Catal Today 300:160–172

Tang J-y, Guo R-t, Pan W-g, Zhou W-g, Huang C-y (2019) Visible light activated photocatalytic behaviour of Eu(III) modified g-C_3N_4 for CO_2 reduction and H_2 evolution. Appl Surf Sci 467–468:206–212

Tuci G, Filippi J, Ba H, Rossin A, Luconi L, Pham-Huu C, Vizza F, Giambastiani G (2018) How to teach an old dog new (electrochemical) tricks: aziridine-functionalized CNTs as efficient electrocatalysts for the selective CO_2 reduction to CO. J Mater Chem A 6:16382–16389

Volokh M, Peng G, Barrio J, Shalom M (2019) Carbon nitride materials for water splitting photoelectrochemical cells. Angew Chem Int Ed 58:6138–6151

Wang X, Maeda K, Thomas A, Takanabe K, Xin G, Carlsoon JM, Domen K, Antonietti M (2009) A metal-free polymeric photocatalyst for hydrogen production from water under visible light. Nat Mater 8:76–80

Wang H, Chen Y, Hou X, Ma C, Tan T (2016) Nitrogen-doped graphenes as efficient electrocatalysts for the selective reduction of carbon dioxide to formate in aqueous solution. Green Chem 18:3250–3256

Wang H, Jia J, Song P, Wang Q, Li D, Min S, Qian C, Wang L, Li YF, Ma C, Wu T, Yuan J, Antonietti M, Ozin GA (2017) Efficient electrocatalytic reduction of CO_2 by nitrogen-doped nanoporous carbon/carbon nanotube membranes: a step towards the electrochemical CO_2 refinery. Angew Chem Int Ed 56:7847–7852

Wang P, Wang S, Wang H, Wu Z, Wang L (2018a) Recent progress on photo-electrocatalytic reduction of carbon dioxide. Part Part Syst Charact 35:1700371–1700396

Wang L, Tong Y, Feng J, Hou J, Li J, Hou X, Liang J (2018b) g-C_3N_4-based films: a rising star for photoelectrochemical water splitting. Sustain Mater Technol 17:e00089–e00109

Wen J, Xie J, Chen X, Li X (2017) A review of g-C_3N_4-based photocatalysts. Appl Surf Sci 391:72–123

Won DH, Chung J, Park SH, Kim E-H, Woo SI (2015) Photoelectrochemical production of useful fuels from carbon dioxide on a polypyrrole-coated p-ZnTe photocathode under visible light irradiation. J Mater Chem A 3:1089–1095

Wu J, Yadav RM, Liu M, Sharma PP, Tiwary CS, Ma L, Zou X, Zhou X-D, Yakobson BI, Lou J, Ajayan PM (2015) Achieving highly efficient, selective, and stable CO_2 reduction on nitrogen-doped carbon nanotubes. ACS Nano 9:5364–5371

Wu J, Liu M, Sharma PP, Yadav RM, Ma L, Yang Y, Zou X, Zhou X-D, Vajtai R, Yakobson BI, Lou J, Ajayan PM (2016a) Incorporation of nitrogen defects for efficient reduction of CO_2 via two-electron pathway on three-dimensional graphene foam. Nano Lett 16:466–470

Wu J, Ma S, Sun J, Gold JI, Tiwary CS, Kim B, Zhu L, Chopra N, Odeh IN, Vajtai R, Yu AZ, Luo R, Lou J, Ding G, Kenis PJA, Ajayan PM (2016b) A metal-free electrocatalyst for carbon dioxide reduction to multi-carbon hydrocarbons and oxygenates. Nat Commun 7:13869–13875

Xie S, Zhang Q, Liu G, Wang Y (2016) Photocatalytic and photoelectrocatalytic reduction of CO_2 using heterogeneous catalysts with controlled nanostructrures. Chem Commun 52:35–59

Xie J, Zhao X, Wu M, Li Q, Wang Y, Yao J (2018) Metal-free fluorine-doped carbon electrocatalyst for CO_2 reduction outcompeting hydrogen evolution. Angew Chem Int Ed 57:9640–9644

Xu J, Kan Y, Huang R, Zhang B, Wang B, Wu K-H, Lin Y, Sun X, Li Q, Centi G, Su D (2016) Revealing the origin of activity in nitrogen-doped nanocarbons towards electrocatalytic reduction of carbon dioxide. Chemsuschem 9:1085–1089

Yang Y, Ajmal S, Zheng X, Zhang L (2018) Efficient nanomaterials for harvesting clean fuels from electrochemical and photoelectrochemical CO_2 reduction. Sustain Energy Fuels 2:510–537

Yao L, Rahmanudin A, Guijarro N, Sivula K (2018) Organic semiconductor based devices for solar water splitting. Adv Energy Mater 8:1802585–1802603

Yongfang L (2015) Organic optoelectronic materials. Conducting polymers, 1st edn. Springer International Publishing, Cham, pp 23–50

Zhang S, Kang P, Ubnoske S, Brennaman MK, Song N, House RL, Glass JT, Meyer TJ (2014) Polyethylenimine-enhanced electrocatalytic reduction of CO_2 to formate at nitrogen-doped carbon nanomaterials. J Am Chem Soc 136:7845–7848

Zhang D, Shi J, Zi W, Wang P, Liu S (2018a) Recent advances in photoelectrochemical applications of silicon materials for solar-to-chemicals conversion. Chemsuschem 10:4324–4341

Zhang B, Zhao T-J, Feng W-J, Liu Y-X, Wang H-H, Su H, Lv L-B, Li X-H, Chen J-S (2018b) Polarized few-layer g-C_3N_4 as metal-free electrocatalyst for highly efficient reduction of CO_2. Nano Res 11:2450–2459

Zheng Y, Zhang W, Li Y, Chen J, Yu B, Wang J, Zhang L, Zhang J (2017) Energy related CO_2 conversion and utilization: advanced materials/nanomaterials, reaction mechanisms and technologies. Nano Energy 40:512–539

Zhu B, Zhang L, Xu D, Cheng B, Yu J (2017) Adsorption investigation of CO_2 on g-C_3N_4 surface by DTF calculation. J CO_2 Util 21:327–335